

Lithium Hexamethyldisilazide-Mediated Ketone Enolization: The Influence of Hindered Dialkyl Ethers and Isostructural Dialkylamines on Reaction Rates and Mechanisms

Pinjing Zhao, Brett L. Lucht, Sarita L. Kenkre, and David B. Collum*

Department of Chemistry and Chemical Biology, Baker Laboratory, Cornell University, Ithaca, New York 14853-1301

dbc6@cornell.edu

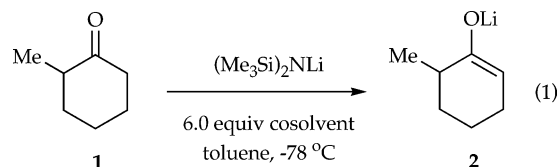
Received July 10, 2003

Mechanistic studies of the enolization of 2-methylcyclohexanone mediated by lithium hexamethyldisilazide (LiHMDS; TMS_2NLi) solvated by hindered dialkyl ethers (ROR') are described. Rate studies using in situ IR spectroscopy show that enolizations in the presence of *i*-Pr₂O, 2,2,5,5-tetramethyltetrahydrofuran, and cineole proceed via dimer-based transition structures $[(\text{TMS}_2\text{NLi})_2(\text{ROR}')(\text{ketone})]^\ddagger$. Comparing the relative solvation energies and the corresponding solvent-dependent activation energies shows that the highly substituted ethers accelerate the enolizations by sterically destabilizing the reactants and stabilizing the transition structures. Comparisons of hindered dialkyl ethers with their isostructural dialkylamines reveal that the considerably higher rates elicited by the amines derive from an analogous relative destabilization of the reactants and relative stabilization of the transition structures.

Introduction

High thermal stability, reactivity, and selectivity combine to make lithium hexamethyldisilazide (LiHMDS) one of the most important Brønsted bases in organic synthesis.^{1,2} These properties also make LiHMDS an excellent template for investigating structure–reactivity relationships within organolithium chemistry. Structural studies of LiHMDS solvated by nearly 100 mono- and bidentate ethers and amines³ provided key insights into lithium ion coordination chemistry and established a firm basis to understand solvent-dependent reactivities and mechanisms.⁴

We began studying how solvation influences the reactivity of LiHMDS by focusing on one of the most important reactions in organolithium chemistry, ketone enolization.¹ Early efforts revealed that poorly coordinating trialkylamines^{4a,5} can cause up to 3000-fold accelerations compared to enolizations in neat toluene (eq 1).⁶ The rates



cosolvent:	none	THF	Et ₃ N
<i>k</i> _{rel} :	1.0	20	3,000

increase with increasing steric demand for a considerable range of amines but fall off sharply using the most hindered amines.⁷ The surprising amine-dependent rates were traced to a dimer-based mechanism in which *destabilizing* interactions in LiHMDS dimer **3** are attenuated in a putative open-dimer-based transition structure **4** (Scheme 1).^{8,9}

(1) For selected examples in which LiHMDS is used on large scale, see: (a) Parsons, R. L., Jr. *Curr. Opin. Drug Discovery Dev.* **2000**, *3*, 783. (b) Kauffman, G. S.; Harris, G. D.; Dorow, R. L.; Stone, B. R. P.; Parsons, R. L., Jr.; Pesti, J. A.; Magnus, N. A.; Fortunak, J. M.; Confalone, P. N.; Nugent, W. A. *Org. Lett.* **2000**, *2*, 3119. (c) Boys, M. L.; Cain-Janicki, K. J.; Doubleday, W. W.; Farid, P. N.; Kar, M.; Nugent, S. T.; Behling, J. R.; Pilipauskas, D. R. *Org. Process Res. Dev.* **1997**, *1*, 233. (d) Ragan, J. A.; Murry, J. A.; Castaldi, M. J.; Conrad, A. K.; Jones, B. P.; Li, B.; Makowski, T. W.; McDermott, R.; Sitter, B. J.; White, T. D.; Young, G. R. *Org. Process Res. Dev.* **2001**, *5*, 498. (e) Rico, J. G. *Tetrahedron Lett.* **1994**, *35*, 6599. (f) DeMattei, J. A.; Leanna, M. R.; Li, W.; Nichols, P. J.; Rasmussen, M. W.; Morton, H. E. *J. Org. Chem.* **2001**, *66*, 3330.

(2) For reviews of structural investigations of lithium amides, see: (a) Gregory, K.; Schleyer, P. v. R.; Snaith, R. *Adv. Inorg. Chem.* **1991**, *37*, 47. (b) Mulvey, R. E. *Chem. Soc. Rev.* **1991**, *20*, 167. (c) Beswick, M. A.; Wright, D. S. In *Comprehensive Organometallic Chemistry II*; Abel, E. W.; Stone, F. G. A., Wilkinson, G., Eds.; Pergamon: New York, 1995; Vol. 1, Chapter 1. (d) Collum, D. B. *Acc. Chem. Res.* **1993**, *26*, 227.

(3) Lucht, B. L.; Collum, D. B. *Acc. Chem. Res.* **1999**, *32*, 1035.

(4) For leading references to structural and mechanistic studies of LiHMDS, see: (a) Lucht, B. L.; Collum, D. B. *J. Am. Chem. Soc.* **1996**, *118*, 2217. (b) Romesberg, F. E.; Collum, D. B. *J. Am. Chem. Soc.* **1992**, *114*, 2112. (c) Romesberg, F. E.; Collum, D. B. *J. Am. Chem. Soc.* **1994**, *116*, 9187. (d) Romesberg, F. E.; Collum, D. B. *J. Am. Chem. Soc.* **1995**, *117*, 2166.

(5) For evidence that the steric hindrance of amines can make them poor ligands for lithium, see ref 4.

(6) (a) Zhao, P.; Collum, D. B. *J. Am. Chem. Soc.* **2003**, *125*, 4008.

(b) Zhao, P.; Collum, D. B. *J. Am. Chem. Soc.*, in press.

(7) For an early suggestion that steric effects are major determinants of solvation, see: Settle, F. A.; Haggerty, M.; Eastham, J. F. *J. Am. Chem. Soc.* **1964**, *86*, 2076.

(8) (a) Remenar, J. F.; Collum, D. B. *J. Am. Chem. Soc.* **1997**, *119*, 5573. (b) Haeffner, F.; Sun, C. Z.; Williard, P. G. *J. Am. Chem. Soc.* **2000**, *122*, 12542. (c) Remenar, J. F.; Collum, D. B. *J. Am. Chem. Soc.* **1998**, *120*, 4081. (d) Remenar, J. F.; Collum, D. B. *J. Am. Chem. Soc.* **1998**, *120*, 4081.

SCHEME 1

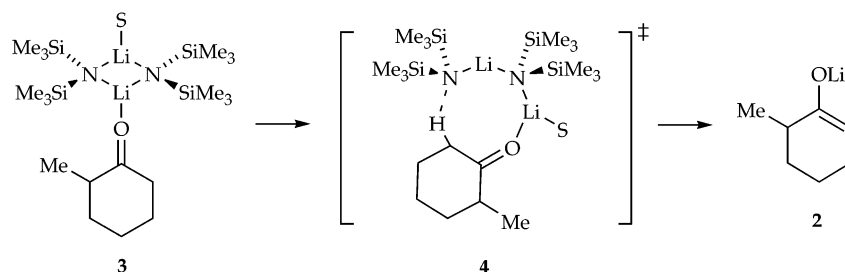
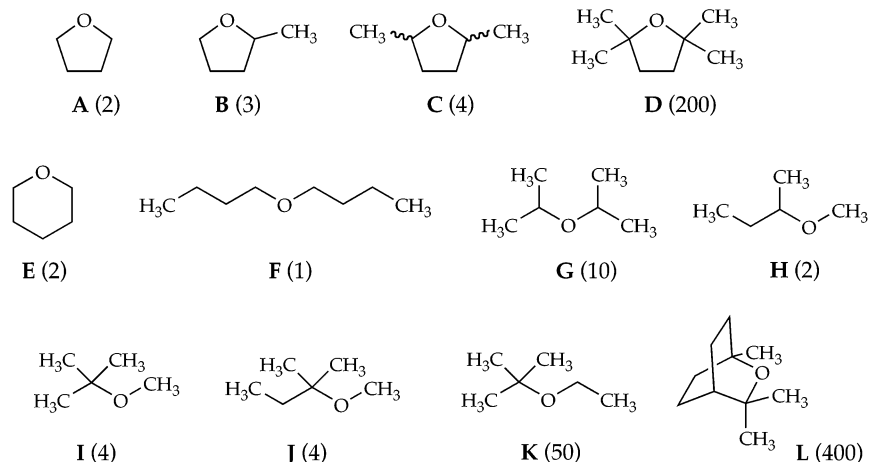


CHART 1. Relative Rate Constants (k_{rel} , in parentheses) for the Enolization of 2-Methylcyclohexanone (1) by LiHMDS (eq 1) in the Presence of 1.5 Equiv of Etheral Ligand in Toluene at $-78\text{ }^{\circ}\text{C}$ ^a



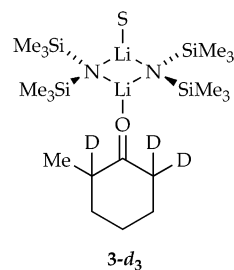
^a The values are relative to enolizations in neat (ether-free) toluene ($k_{rel} = 1$).

We now describe investigations of LiHMDS-mediated ketone enolizations that were guided by two central questions: Is there an analogous dimer-based enolization for LiHMDS in the presence of hindered ethers, and, if so, how do the influences of amines and ethers differ?

Results

Kinetics: General Methods. Ketone **1** was added to LiHMDS in hydrocarbon/ R_2O mixtures at $-78\text{ }^{\circ}\text{C}$. In situ IR spectroscopy¹⁰ reveals that **1** (1722 cm^{-1}) is quantitatively converted to LiHMDS–ketone complexes ($1706\text{--}1708\text{ cm}^{-1}$) shown to be of general structure **3** by ^6Li and ^{15}N NMR spectroscopies (Supporting Information).^{3,6} Pseudo-first-order conditions were established by maintaining low concentrations of ketone **1** ($0.004\text{--}0.01\text{ M}$) and high, yet adjustable, concentrations of recrystallized¹¹ LiHMDS ($0.05\text{--}0.40\text{ M}$) and ether ($0.15\text{--}1.80\text{ M}$) in toluene as the cosolvent. At such low ketone concentrations, only dimer **3**, bearing a single coordinated ketone, is formed.^{6,10a,12–14} In all cases, the loss of **3** (or the less reactive deuterated analogue **3-d₃**)¹⁵ follows first-order decays to >5 half-lives. The resulting pseudo-first-

order rate constants (k_{obsd}) are independent of the initial ketone concentration ($0.004\text{--}0.04\text{ M}$), confirming the first-order dependence on the concentration of **3**. Zeroing the IR baseline and monitoring a second injection afford no significant change in the rate constant, showing that conversion-dependent autocatalysis or autoinhibition are unimportant under these conditions.¹⁶ Comparisons of **3** and **3-d₃** provided large kinetic isotope effects, confirming rate-limiting proton transfers.^{17–19}



Relative Rate Constants. The rate constants for enolization depend on the structure of the etheral solvent as listed in parentheses in Chart 1. The rate

(9) (a) Remenar, J. F.; Lucht, B. L.; Kruglyak, D.; Romesberg, F. E.; Gilchrist, J. H.; Collum, D. B. *J. Org. Chem.* **1997**, *62*, 5748. (b) Williard, P. G.; Liu, Q.-Y. *J. Am. Chem. Soc.* **1993**, *115*, 3380.

(10) (a) Sun, X.; Collum, D. B. *J. Am. Chem. Soc.* **2000**, *122*, 2452. (b) Review: Rein, A. J.; Donahue, S. M.; Pavlosky, M. A. *Curr. Opin. Drug Discovery Dev.* **2000**, *3*, 734.

(11) Romesberg, F. E.; Bernstein, M. P.; Gilchrist, J. H.; Harrison, A. T.; Fuller, D. J.; Collum, D. B. *J. Am. Chem. Soc.* **1993**, *115*, 3475.

(12) Williard, P. G.; Liu, Q. Y.; Lochmann, L. *J. Am. Chem. Soc.* **1992**, *114*, 348.

(13) For leading references and recent examples of detectable organolithium–substrate complexation, see: (a) Klumpp, G. W. *Recl. Trav. Chim. Pays-Bas* **1986**, *105*, 1. (b) Andersen, D. R.; Faibish, N. C.; Beak, P. *J. Am. Chem. Soc.* **1999**, *121*, 7553. Also, see ref 4.

(14) For a general discussion of ketone–lithium complexation and related ketone–Lewis acid complexation, see: Shambayati, S.; Schreiber, S. L. In *Comprehensive Organic Synthesis*; Trost, B. M., Fleming, I., Eds.; Pergamon: New York, 1991; Vol. 1, p 283.

(15) Peet, N. P. *J. Labelled Compd.* **1973**, *9*, 721.

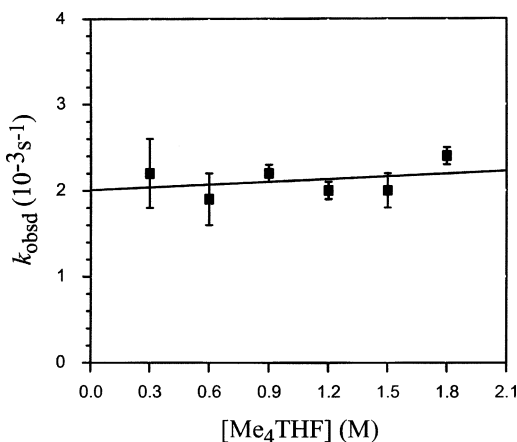
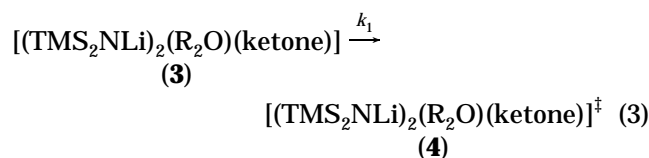


FIGURE 1. Plot of k_{obsd} vs $[\text{Me}_4\text{THF}]$ in toluene for the enolization of **1** (0.004 M) by LiHMDS (0.10 M) at $-78\text{ }^\circ\text{C}$. The line depicts an unweighted least-squares fit to $k_{\text{obsd}} = ax + b$ ($a = (1 \pm 2) \times 10^{-4}$, $b = (2.0 \pm 0.2) \times 10^{-3}$).

constants do not, however, depend on the concentration of the solvent. This behavior is often emblematic of the dimer-based mechanism in Scheme 1. Casual inspection reveals that the accelerations caused by even the most hindered ethers are modest when compared with the dramatic (up to 3000-fold) accelerations observed for Et_3N and related trialkylamines.⁶

Rate Laws: Hindered Dialkyl Ethers. Detailed rate studies of LiHMDS-mediated enolizations (eq 1) in the presence of commercially available hindered ethers 2,2,5,5-tetramethyltetrahydrofuran (Me_4THF , **D**), *i*-Pr₂O (**G**), and cineole (**L**) provided analogous rate laws; the results for Me_4THF are representative. Plots of k_{obsd} vs Me_4THF concentration (Figure 1) and k_{obsd} vs LiHMDS²⁰ concentration (Figure 2) both display zeroth-order dependencies. The rate law (eq 2) indicates that the observable ether-solvated complex **3** neither gains nor loses a molecule of Me_4THF or a LiHMDS subunit on proceeding to the rate-limiting transition structure,²¹ consistent with the dimer-based mechanism described generically in eq 3 and with structural details in Scheme 1.

$$-d[\mathbf{3}]/dt = k_1[\mathbf{3}] \quad (2)$$



(16) (a) Seebach, D. *Angew. Chem., Int. Ed. Engl.* **1988**, *27*, 1624. (b) Sun, X.; Collum, D. B. *J. Am. Chem. Soc.* **2000**, *122*, 2459. (c) McGarrity, J. F.; Ogle, C. A. *J. Am. Chem. Soc.* **1984**, *107*, 1810. (d) Thompson, A.; Corley, E. G.; Huntington, M. F.; Grabowski, E. J. J.; Remenar, J. F.; Collum, D. B. *J. Am. Chem. Soc.* **1998**, *120*, 2028. (e) Hall, P.; Gilchrist, J. H.; Harrison, A. T.; Fuller, D. J.; Collum, D. B. *J. Am. Chem. Soc.* **1991**, *113*, 9571.

(17) Isotope effects for LiHMDS-mediated ketone enolizations: (a) Held, G.; Xie, L. F. *Microchem. J.* **1997**, *55*, 261. (b) Xie, L. F.; Saunders, W. H. *J. Am. Chem. Soc.* **1991**, *113*, 3123.

(18) The isotope effects fall within the range $k_H/k_D = 10\text{--}20$ as noted in Supporting Information.

(19) The regioselectivity indicated in eq 1 was shown to be $>20:1$ by trapping with $\text{Me}_3\text{SiCl}/\text{Et}_3\text{N}$ mixtures.

(20) The concentration of the lithium amide, although expressed in units of molarity, refers to the concentration of the monomer unit (normality).

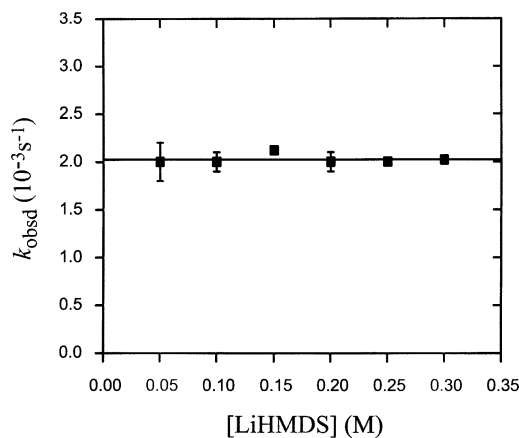
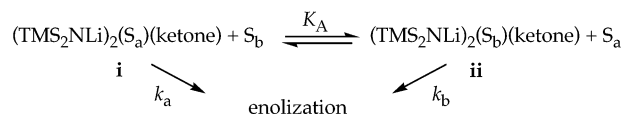


FIGURE 2. Plot of k_{obsd} vs $[\text{LiHMDS}]$ for the enolization of **1** (0.004 M) in 1.2 M Me_4THF /toluene at $-78\text{ }^\circ\text{C}$. The line depicts an unweighted least-squares fit to $k_{\text{obsd}} = ax + b$ ($a = -(1 \pm 3) \times 10^{-5}$, $b = (2.03 \pm 0.05) \times 10^{-3}$).

SCHEME 2



Correlation of Rates and Solvent Binding Constants. To show that the modest rate accelerations correlate inversely with solvent-binding constants, we used a variant²² of a Job plot²³ to construct a thermochemical description of solvation as follows.

Enolizations of **1** by LiHMDS in mixtures of two solvents, S_A and S_B , at fixed molarity ($[\text{S}_A] + [\text{S}_B] = \text{constant}$) are depicted in Scheme 2. The rate constants measured in the presence of each solvent alone provide the free energies of activation, $\Delta G^\ddagger(\text{S}_A)$ and $\Delta G^\ddagger(\text{S}_B)$. Equation 4 describes k_{obsd} in terms of mechanistic constants and mole fractions²⁴ of S_A and S_B (X_A and $1 - X_A$, respectively). The value of K_A provides a measure of the relative free energies of the two ground states, $\Delta G^\circ_{\text{GS}}$, corresponding to dimer-based complexes **i** and **ii**. In turn, $\Delta G^\ddagger(\text{S}_A)$, $\Delta G^\ddagger(\text{S}_B)$, and $\Delta G^\circ_{\text{GS}}$ provide the difference in the transition-state energies, $\Delta G^\circ_{\text{TS}}$. Results from a number of binary comparisons are summarized in Table 1 and are discussed in the context of the generic free energy diagram illustrated in Figure 3.

By example, a plot of k_{obsd} versus the mole fraction of *i*-Pr₂O²⁴ for the enolization in mixtures of *i*-Pr₂O and *i*-Bu₂O is shown in Figure 4. The upward curvature in Figure 4 is emblematic of a higher rate correlating with the poorly coordinating solvent and is consistent with the steric acceleration noted in previous studies of LiHMDS/ R_3N -mediated enolizations.⁶ The nonlinear least-squares fit to eq 4 affords the free energies listed in Table 1, which

(21) Edwards, J. O.; Greene, E. F.; Ross, J. *J. Chem. Educ.* **1968**, *45*, 381.

(22) For a closely related application of this particular variant of the Job plot, see refs 6b and 8a.

(23) (a) Job, P. *Ann. Chim.* **1928**, *9*, 113. For more recent examples and leading references, see: (b) Huang, C. Y. *Methods Enzymol.* **1982**, *87*, 509. (c) Hubbard, R. D.; Horner, S. R.; Miller, B. L. *J. Am. Chem. Soc.* **2001**, *123*, 5810. (d) Potluri, V.; Maitra, U. *J. Org. Chem.* **2000**, *65*, 7764.

(24) Mole fraction is defined as the fraction of the total number of moles of coordinating solvent: $[\textit{i}\text{-Pr}_2\text{NH}] + [\textit{i}\text{-Pr}_2\text{O}] = 1.2\text{ M}$.

TABLE 1. Free Energies for the LiHMDS-Mediated Enolization of 1 in Binary Solvent Mixtures (Scheme 2, Figure 3)^a

entry	S _a	S _b	$\Delta G^\ddagger(S_a)$	$\Delta G^\ddagger(S_b)$	ΔG°_{GS}	ΔG°_{TS}
1 ^b	<i>i</i> -Bu ₂ O	<i>i</i> -Pr ₂ O	15.4 ± 0.1	14.9 ± 0.1	0.3 ± 0.1	-0.2 ± 0.1
2	<i>i</i> -Pr ₂ O	Me ₄ THF	14.9 ± 0.1	13.5 ± 0.1	0.27 ± 0.08	-1.1 ± 0.1
3	<i>i</i> -Bu ₂ O	Me ₄ THF	15.4 ± 0.2	13.5 ± 0.1	0.83 ± 0.02	-1.1 ± 0.2
4	<i>i</i> -Pr ₂ O	<i>i</i> -Pr ₂ NH	14.9 ± 0.1	13.0 ± 0.1	0.79 ± 0.02	-1.1 ± 0.1
5	<i>i</i> -PrOEt	<i>i</i> -PrNHET	15.3 ± 0.1	14.0 ± 0.1	0.04 ± 0.09	-1.28 ± 0.09

^a Conditions: [LiHMDS] = 0.10 M; [solvent]_{total} = 1.2 M; toluene cosolvent. ^b Nearly equivalent rates attenuates the accuracy of the method.

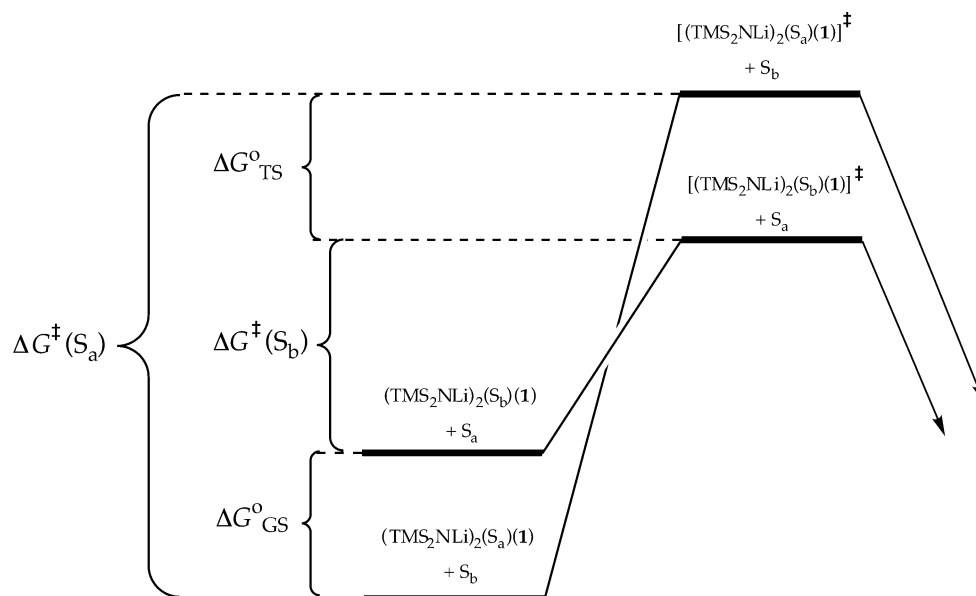
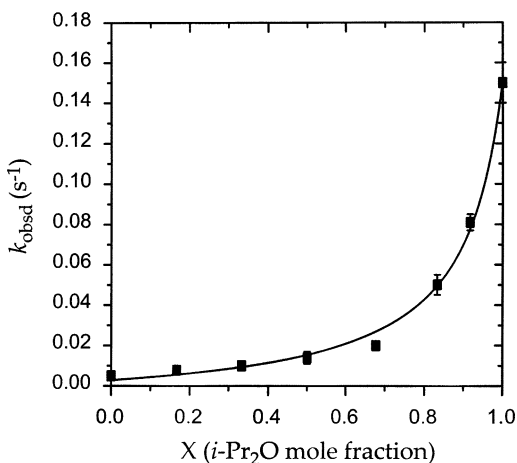
**FIGURE 3.** Thermochemical description of LiHMDS-mediated enolizations in binary solvent mixtures (Scheme 2, Table 1).

FIGURE 4. Plot of k_{obsd} vs *i*-Pr₂O mole fraction in *i*-Pr₂O/*i*-Bu₂O²⁴ for the enolization of **1** (0.004 M) by LiHMDS (0.10 M) at -40 °C. The curve depicts an unweighted least-squares fit to $y = (a + bx)/(1 + cx)$, where $a = (2 \pm 2) \times 10^{-3}$, $b = (1.2 \pm 0.3) \times 10^{-2}$, $c = -0.905 \pm 0.009$. $K_A(i\text{-Pr}_2\text{O}/i\text{-Bu}_2\text{O}) = 1 + c = 0.095 \pm 0.009$.

are expressed by the free energy diagram shown in Figure 3. As expected, the acceleration reflected by $\Delta G^\ddagger(i\text{-Pr}_2\text{O}) < \Delta G^\ddagger(i\text{-Bu}_2\text{O})$ derives in part from a relative destabilization of the reactant (reflected in ΔG°_{GS}) by the sterically more demanding ligand. It was altogether unexpected, however, that the more sterically congested ligand would also impart a net *stabilization* of the open-dimer-based transition structure (reflected by the nega-

tive ΔG°_{TS}). Additional binary comparisons listed in Table 1 also prove instructive.

A plot of k_{obsd} vs the mole fraction of Me₄THF²⁴ for the LiHMDS-mediated enolizations in Me₄THF/*i*-Pr₂O mixtures (Figure 5) displays a slight upward curvature consistent with nearly identical solvation of the reactants ($\Delta G^\circ_{GS} = 0$). Thus, the approximate 20-fold higher rate for the LiHMDS/Me₄THF-mediated enolization derives almost entirely from a net stabilization of the transition structure. The nonlinear least-squares fit to the data affords the free energies listed in Table 1 (Table 1, entry 2). We will discuss the effects of increasing substitution within the etheral ligand on the reactant and transition structure in the context of competing steric and electronic effects.

$$k_{\text{obsd}} = [k_b + (k_a - k_b K_A) X_a / K_A] / [1 + (1 - K_A) X_a / K_A] \quad (4)$$

such that $X_a = [S_a] / ([S_a] + [S_b])$ and $([S_a] + [S_b]) =$ constant molarity.

The veracity of the data in Table 1 can be supported by simple cross checks. By example, the binary comparisons of *i*-Bu₂O vs *i*-Pr₂O (entry 1) and *i*-Pr₂O vs Me₄THF (entry 2) allow one to predict the result from a comparison of *i*-Bu₂O vs Me₄THF and then compare it to the experimental result (entry 3), showing strong self-consistency within a reasonable experimental error.

Comparison of R₂NH vs R₂O. Table 2 lists relative rate constants for a select group of isostructural dialkyl-

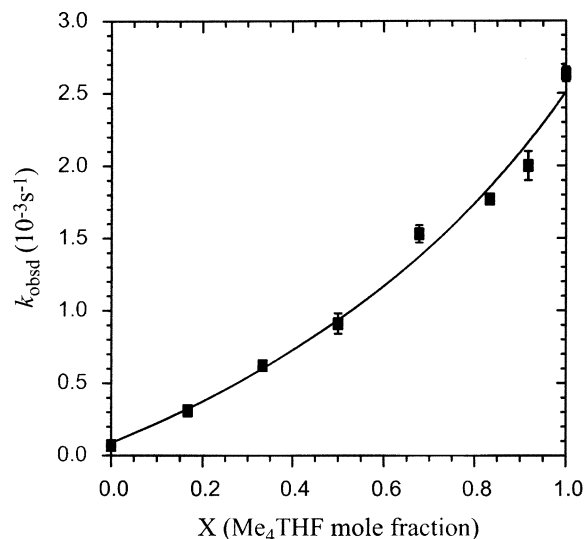


FIGURE 5. Plot of k_{obsd} vs Me_4THF mole fraction in $\text{Me}_4\text{THF}/i\text{-Pr}_2\text{O}^{24}$ for the enolization of **1** (0.004 M) by LiHMDS (0.10 M) at -78°C . The curve depicts an unweighted least-squares fit to $y = (a + bx)/(1 + cx)$, where $a = (9 \pm 9) \times 10^{-5}$, $b = (1.3 \pm 0.3) \times 10^{-3}$, $c = -0.5 \pm 0.1$. $K_A(\text{Me}_4\text{THF}/i\text{-Pr}_2\text{O}) = 1 + c = 0.5 \pm 0.1$.

TABLE 2. Relative Rates (k_{rel}) for the Enolization by LiHMDS Solvated by Isostructural Dialkylamines (R_1NHR_2) and Dialkyl Ethers (R_1OR_2)

R_1XR_2	$k_{\text{amine}}/k_{\text{ether}}$
$\text{R}_1 = \text{R}_2 = i\text{-Bu}$	2
$\text{R}_1 = \text{R}_2 = i\text{-amyl}$	10
$\text{R}_1 = \text{Et}, \text{R}_2 = i\text{-Pr}$	35
$\text{R}_1 = \text{R}_2 = i\text{-Pr}$	170
$\text{R}_1 = \text{R}_2 = s\text{-Bu}$	60

^a Enolization rates were measured with 0.1 M LiHMDS, 0.004 M 2-methylcyclohexanone (**1**), and 1.2 M ligand in a toluene solution at -78°C .

amines and dialkyl ethers. Comparing the hindered $i\text{-Pr}_2\text{O}/i\text{-Pr}_2\text{NH}$ pair reveals a markedly greater acceleration by the $i\text{-Pr}_2\text{NH}$. Figure 6 illustrates the rate constants measured as a function of solvent mole fraction.²⁴ Once again, the free energies listed in Table 1 are qualitatively consistent with the free-energy diagram in Figure 3. In particular, the higher rates using $i\text{-Pr}_2\text{NH}$ compared to the isostructural $i\text{-Pr}_2\text{O}$ derive from a combination of relative destabilization of the hindered lithium amide dimer **3** and relative stabilization of open-dimer-based transition structure **4**. A different result is obtained by comparing $i\text{-PrOEt}$ and $i\text{-PrNHEt}$ (Figure 7). The higher rates for $i\text{-PrNHEt}$ derive almost entirely from stabilization of the transition state ($\Delta G_{\text{CS}}^\circ = 0$). The third and possibly most aberrant result derives from a comparison of $i\text{-Bu}_2\text{O}$ and $i\text{-Bu}_2\text{NH}$ in which nearly equivalent rates and binding constants are observed; $\Delta G_{\text{CS}}^\circ$ and $\Delta G_{\text{TS}}^\circ$ are too small to measure using this method.

Discussion

Conventional wisdom suggests that the LiHMDS-mediated enolizations of ketones are accelerated by strongly coordinating ligands due to intervening deaggregation.²⁵ Nonetheless, previous investigations showed

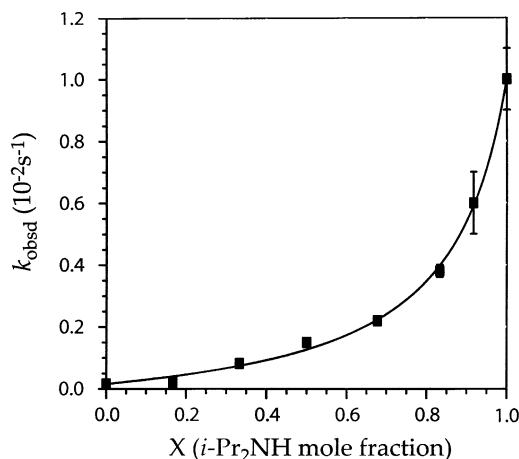


FIGURE 6. Plot of k_{obsd} vs $i\text{-Pr}_2\text{NH}$ mole fraction in $i\text{-Pr}_2\text{NH}/i\text{-Pr}_2\text{O}^{24}$ for the enolization of **1** (0.004 M) by LiHMDS (0.10 M) at -78°C . The curve depicts an unweighted least-squares fit to $y = (a + bx)/(1 + cx)$, where $a = (1 \pm 1) \times 10^{-5}$, $b = (1.2 \pm 0.2) \times 10^{-3}$, $c = -0.871 \pm 0.008$. $K_A(i\text{-Pr}_2\text{NH}/i\text{-Pr}_2\text{O}) = 1 + c = 0.129 \pm 0.008$.

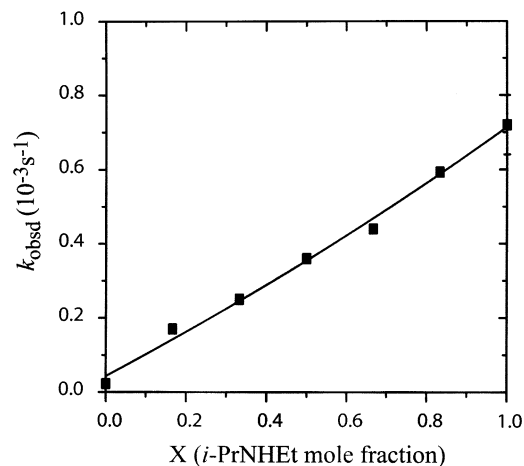


FIGURE 7. Plot of k_{obsd} vs $i\text{-PrNHEt}$ mole fraction in $i\text{-PrNHEt}/i\text{-PrOEt}^{24}$ for the enolization of **1** (0.004 M) by LiHMDS (0.10 M) at -78°C . The curve depicts an unweighted least-squares fit to $y = (a + bx)/(1 + cx)$, where $a = (4 \pm 2) \times 10^{-5}$, $b = (5.7 \pm 0.9) \times 10^{-4}$, $c = -0.1 \pm 0.1$. $K_A(i\text{-PrNHEt}/i\text{-PrOEt}) = 1 + c = 0.9 \pm 0.1$.

that the ketone enolization in eq 1 is dramatically accelerated by *poorly* coordinating trialkylamines due to the intervention of a dimer-based pathway (Scheme 1).⁶ The correlation of high rates with solvation of LiHMDS by hindered di- and trialkylamines was traced to steric relief that occurs when the reaction proceeds from the congested dimer-based LiHMDS–ketone complex **3** to the relatively less congested⁸ open-dimer-based transition structure **4** as depicted using the generic free-energy diagram in Figure 8.^{26,27} These results offer a tribute to

(25) Collum, D. B. *Acc. Chem. Res.* **1992**, *25*, 448.

(26) The relative solvation energies of the reactant ($\Delta G_{\text{CS}}^\circ$) and transition structure ($\Delta G_{\text{TS}}^\circ$) for a series of amines display a linear free energy relationship of the form:

$$\Delta G_{\text{TS}}^\circ = 0.6\Delta G_{\text{CS}}^\circ$$

The high linearity and simplicity of the relationship is remarkable given that specific through-space (van der Waals) interactions can render steric effects very complex.²⁷

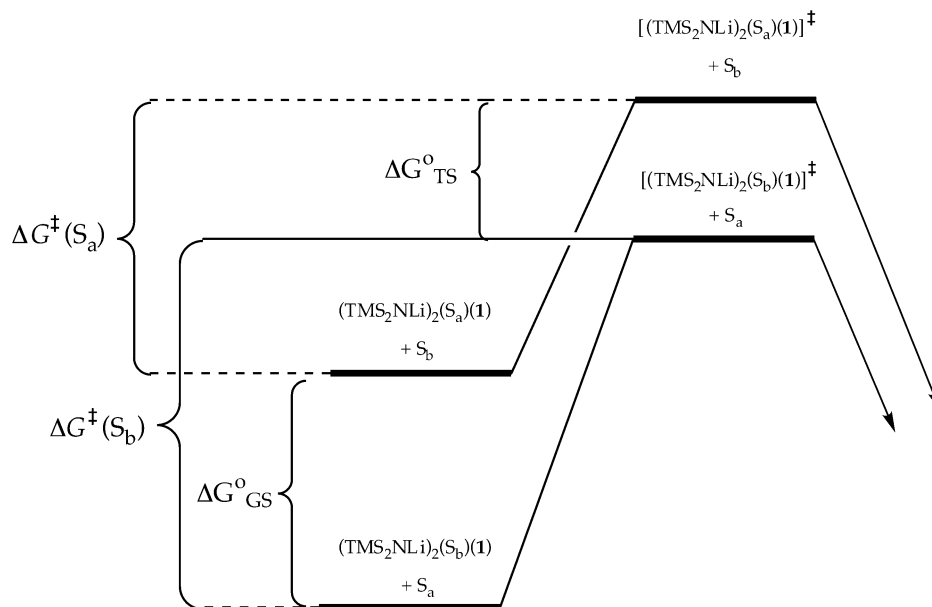


FIGURE 8. Thermochemical description of amine-mediated enolizations noted previously.^{7a}

computational chemistry in that a facile open-dimer-based ketone enolization and an accompanying steric acceleration emerged quite unexpectedly from semiempirical calculations in 1992.⁴

We prefaced the current study with two questions: (1) Is there an analogous dimer-based enolization for LiHMDS in the presence of hindered ethers, and (2) if so, how do the influences of amines and ethers differ? Rate studies reveal that LiHMDS solvated by sterically demanding ethers, Me₄THF (**D**), *i*-Pr₂O (**G**), and cineole (**L**), enolizes ketone **1** via the dimer-based pathway shown in Scheme 1. The accelerations shown in Chart 1, however, are muted compared to the 3000-fold acceleration observed for LiHMDS/Et₃N mixtures. Do the attenuated rates for the ethers simply reflect the lesser steric demands of even the most hindered dialkyl ethers when compared with simple trialkylamines? To address this point, we turned to a variant²² of a Job plot²³ to correlate the ligand-dependent rates with the steric and electronic demands of the coordinated solvent. For example, a plot of k_{obsd} vs mole fraction of *i*-Pr₂O in *i*-Pr₂O/*i*-Bu₂O mixtures (Figure 4) afforded the thermochemical data in Table 1 (entry 1) and the accompanying free-energy diagram depicted generically in Figure 3. The higher rates for LiHMDS solvated by *i*-Pr₂O derive from a destabilization of the reactant dimer as reflected by $\Delta G^{\circ}_{\text{GS}}$. Surprisingly, however, the more sterically demanding *i*-Pr₂O also imparts a net *stabilization* of the open-dimer-based transition structure. Although we were initially tempted to ascribe the odd reversal in solvation to the unusual steric demands of isobutyl groups noted,^{4a,6b} the same pattern, a positive $\Delta G^{\circ}_{\text{GS}}$ and a negative $\Delta G^{\circ}_{\text{TS}}$, observed for other binary comparisons of hindered ethers (Table 1) suggests a greater generality.

Dialkylamines show more dramatic accelerations that appear to derive from similar effects. Thus, the sterically demanding *i*-Pr₂NH accelerates the enolization when compared with the isostructural *i*-Pr₂O by destabilizing

the reactant and stabilizing the transition structure. Once again, however, the mechanistic picture is not altogether simple. Comparison of less hindered isostructural ligands *i*-PrOEt and *i*-PrHNEt (Table 1, entry 6) reveals that *i*-PrHNEt accelerates the enolization almost entirely due to a net stabilization of the transition structure.

Competing steric effects that are dominant in the ground state and electronic effects that can be dominant in the transition state offer an adequate model for the solvent effects as follows.

(1) Steric Effects. Trialkylamines are functionally larger than even the most hindered dialkyl ethers since ethers coordinated to lithium are trigonal planar at oxygen²⁸ whereas the corresponding amines are necessarily tetrahedral at nitrogen²⁹ (cf. **5** and **6**). Because open dimers and open-dimer-based transition structures are suggested to be less congested than the cyclic dimers,^{4b} extremely hindered ligands such as trialkylamines markedly destabilize the congested dimeric reactant **3** more than the open-dimer-based transition structure **4**, resulting in sterically driven accelerations. By contrast, the sterically less demanding dialkyl ethers and their dialkylamine counterparts should display attenuated steric accelerations and be nearly indistinguishable *provided that the alkyl groups are not large*.^{4a} Apparently, the smallest ligands studied, *i*-PrNHet and *i*-PrOEt, are below what Brown refers to as the “minimum steric threshold”³⁰ as evidenced by the absence of measurable differences in the energies of the reactants.^{4a}

(2) Electronic Effects. Cyclic dimers of lithium amides appear to be less electrophilic (toward coordinating ligands) than their open dimer or monomer counterparts.^{3,4b,8a,31} Therefore, increased Lewis basicity would preferentially stabilize the open-dimer-based transition

(28) Chakrabarti, P.; Dunitz, J. D. *Helv. Chim. Acta* **1982**, *64*, 1482.

(29) Impey, R. W.; Sprik, M.; Klein, M. L. *J. Am. Chem. Soc.* **1987**, *109*, 5900.

(30) Choi, M.-G.; Brown, T. L. *Inorg. Chem.* **1993**, *32*, 1548.

(31) Ramirez, A.; Collum, D. B. *J. Am. Chem. Soc.* **1999**, *121*, 11114.

(27) Brown, T. L.; Lee, K. J. *Coord. Chem. Rev.* **1993**, *128*, 89.

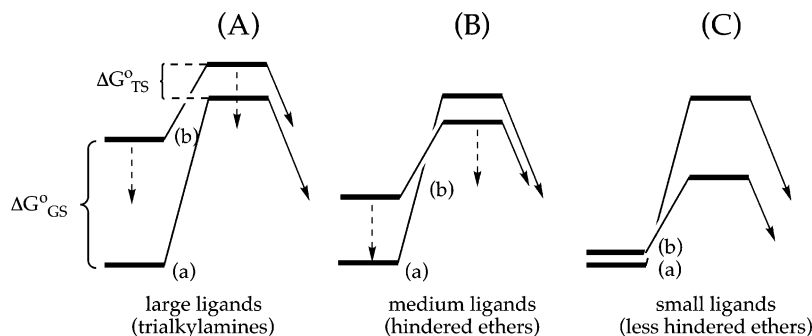
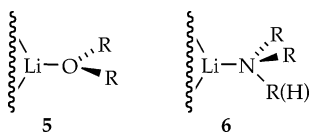


FIGURE 9. Effect of decreasing steric demands of the coordinating ligand on the relative activation energies. Curve a corresponds to a benchmark dimer solvated by an unhindered ethereal ligand. Curve b corresponds to more highly substituted ether or amine. The dotted arrows indicate decreasing steric demands of the more congested solvate.



structures. In addition, the functional Lewis basicity of a ligand depends on a number of factors, including (a) the steric effects noted above, (b) the electrophilicity of the Lewis acid,³² (c) inductive electron donation resulting from substitution on the alkyl groups of the Lewis base (Et versus *i*-Pr),³² and (d) the inherent nucleophilicity of the coordinating atom (N vs O).³⁴ Although the steric demands of Me₄THF are a little unclear, the stabilization of the transition structure due to putative electronic effects is consistent with the inherently high Lewis basicity of tetrahydrofurans.³⁵ In the absence of mitigating steric effects, the Lewis basicity of the ligand should be greater for amines than for ethers³⁴ and should be enhanced by increased substitution on the ligands due to inductive electron donation.³³

By placing the thermochemical depictions proximate (Figure 9), we have constructed a reasonably self-consistent model that serves as a useful mnemonic. For the most hindered ligands, electronic stabilizations of the transition structures are obscured by dominant steric effects in the congested cyclic dimer reactants (Figure 9A). As the steric influences on ΔG°_{GS} and ΔG°_{TS} decrease (indicated by the dotted arrows), the electronic biases favoring the open-dimer-based transition structures become observable (Figure 9B). Under these circumstances, dialkylamines coordinate to the open-dimer-based transition structure more strongly than do dialkyl ethers and substituted ethers bind more strongly than lesser substituted ethers. As the ligands fall below the minimum steric threshold, steric effects localized primarily in the reactant disappear and electronic effects influential in

the open-dimer-based transition structure become dominant (Figure 9C). Further removal of substituents would not influence the steric environment but would decrease the stabilization of the transition structure.

There is an outlying data point, however, we simply do not understand; *i*-Bu₂NH and *i*-Bu₂O were found to be nearly indistinguishable not only in the ground state but also in the transition state. Although equivalent binding in the ground state was anticipated from previous spectroscopic studies,^{4a} it is unclear why the enhanced basicity of the amine does not cause a pronounced stabilization of the transition structure.

Summary and Conclusions

Previous work showed that LiHMDS solvated by di- and trialkylamines effects ketone enolization via a sterically accelerated dimer-based enolization shown in Scheme 1.⁶ Analogous accelerations by hindered dialkyl ethers are traced to sterically derived destabilization of the reactant in conjunction with stabilization of the transition structure due to putative electronic effects. In general, however, the ethers are not sterically demanding enough to elicit high reactivities. Dialkylamines also destabilize the reactant and stabilize the transition structures when compared with the hindered ethers, eliciting higher overall rates.

In the most general sense, increasing the reactivities of lithium amides, whether through amine or ether additives, is potentially important in synthesis. Although the trialkylamines impart the largest accelerations, the ethers may be more appropriate if subsequent reactions use highly reactive electrophiles that can N-alkylate secondary amines. Most importantly, however, enolates solvated by poorly coordinating ligands may display interesting reactivities.

Experimental Section

Reagents and Solvents. Amines and hydrocarbons were routinely distilled by vacuum transfer from blue or purple solutions containing sodium benzophenone ketyl. The hydrocarbon stills contained 1% tetraglyme to dissolve the ketyl. ⁶Li metal (95.5% enriched) was obtained from Oak Ridge National Laboratory. The LiHMDS, [⁶Li]LiHMDS, and [⁶Li,¹⁵N]LiHMDS were prepared and purified as described.¹¹ Ketone **1-d₃** has been prepared as described.¹⁵ Air- and moisture-sensitive materials were manipulated under argon or nitrogen using standard glovebox, vacuum line, and syringe techniques.

(32) (a) Ivanova, S. M.; Nolan, B. G.; Kobayashi, Y.; Miller, S. M.; Anderson, O. P.; Strauss, S. H. *Chem.-Eur. J.* **2001**, *7*, 503. (b) Reed, C. A. *Acc. Chem. Res.* **1998**, *31*, 133.

(33) (a) Baeten, A.; De Proft, F.; Langenaeker, W.; Geerlings, P. *THEOCHEM* **1994**, *112*, 203. (b) Safi, B.; Choho, K.; De Proft, F.; Geerlings, P. *Chem. Phys. Lett.* **1999**, *300*, 85. (c) Headley, A. D. *J. Org. Chem.* **1991**, *56*, 3688.

(34) (a) March, J. *Advanced Organic Chemistry*; Wiley: New York, 1992; Chapter 8. (b) Gutmann, V. *The Donor-Acceptor Approach to Molecular Interactions*; Plenum: New York, 1978. (c) Marcus, Y. *J. Solution Chem.* **1984**, *13*, 599. (d) Kaufmann, E.; Gose, J.; Schleyer, P. v. R. *Organometallics* **1989**, *8*, 2577.

(35) Berthelot, M.; Besseau, F.; Laurence, C. *Eur. J. Org. Chem.* **1940**, *5*, 925.

NMR Spectroscopic Analyses. Samples were prepared, and the ^6Li , ^{15}N , and ^{13}C NMR spectra were recorded as described elsewhere.⁶ The LiHMDS samples containing both ketone **1** and ethers were prepared using a specific protocol designed to minimize unwanted enolization.⁶

IR Spectroscopic Analyses. In situ IR spectra were recorded using a 30-bounce silicon-tipped probe using fully established procedures.^{10a}

Acknowledgment. We thank the National Institutes of Health for direct support of this work as well as Dupont Pharmaceuticals (Bristol-Myers Squibb), Merck Research Laboratories, Pfizer, Aventis, R. W.

Johnson, and Schering-Plough for indirect support. P.Z. thanks Boehringer-Ingelheim for a fellowship. We also acknowledge the National Science Foundation Instrumentation Program (CHE 7904825 and PCM 8018643), the National Institutes of Health (RR02002), and IBM for support of the Cornell Nuclear Magnetic Resonance Facility.

Supporting Information Available: NMR spectra and rate data. This material is available free of charge via the Internet at <http://pubs.acs.org>.

JO030221Y